

Electronic Spectroscopy of the Titanium Centers in Titanium Silicalite

Allison S. Soutl, Duke D. Pooré, Elizabeth I. Mayo, and A. E. Stiegman*

Department of Chemistry and The Materials Research and Technology Center (MARTECH),
Florida State University, Tallahassee, Florida 32306

Received: July 25, 2000; In Final Form: November 15, 2000

Studies of the electronic structure of titanium centers in titanium silicalite (TS-1) catalytic materials were carried out using electronic absorption and emission spectroscopy. A long-lived phosphorescent excited state with an emission maximum at 490 nm in the near UV was unambiguously assigned to the titanium. Resolved in the emission envelope was vibronic structure in 965 cm^{-1} mode, which corresponds to the Si–O–Ti stretching mode in TS-1. The lowest energy excited state is significantly lower in energy than was previously suggested by diffuse reflectance absorption spectroscopy. Emission excitation spectra indicate that, contrary to previous assertions, there are electronic transitions throughout the spectral region from ~ 23000 to 48000 cm^{-1} . These observations bring into question long-standing structural arguments for the coordination of titanium in the silicalite lattice that have been made using electronic spectroscopy.

Introduction

Binary titania–silica oxides have elicited a great deal of interest due to their diverse and useful properties. For example, amorphous titania–silica glass, with titania concentrations of ~ 7 – 8% , is produced commercially for its extremely low coefficient of thermal expansion.¹ Conversely, crystalline titania silicalite zeolites (TS-1) have been found to be highly active and selective catalysts for, among other reactions, the oxidation of phenol to catechol and hydroquinone.^{2,3} The properties of these materials are due to the presence of titanium sites dispersed in the silica matrix. The nature of these sites and how they give rise to the useful properties exhibited by these materials is still unclear. For this reason, a number of studies utilizing a variety of spectroscopic techniques have been carried out to elucidate the coordination geometry and the electronic and photophysical properties of the titanium active sites as they reside in the matrix. Specifically, in the case of TS-1, electronic spectroscopy, collected by diffuse reflectance techniques or through photoemission, has been used to establish the coordination geometry of the titanium site, identify the number of active sites present, and identify the presence of extraframework titania in the final material.^{2–4}

We report here a detailed study of the electronic spectroscopy of the titanium centers in TS-1, using both emission and diffuse reflectance electronic spectroscopies. The results of this study yield insights into the electronic structure and excited-state properties of the reactive titanium site. They also provide a quantitative assessment and a critical reappraisal of the structural arguments for tetrahedral coordination of the titanium thought to be supported by electronic spectroscopy.

Experimental Section

Synthesis. Silicalite and TS-1 were made by published procedures.^{5,6} In a typical preparation, 5.0 g of titanium isopropoxide (Aldrich, 99.999%) was added dropwise to 48.4 g of tetraethyl orthosilicate (Aldrich, 99.999%) under vigorous stirring and a constant flow of nitrogen. The solution was heated

to $35\text{ }^\circ\text{C}$ for 30 min while being stirred and then cooled to $0\text{ }^\circ\text{C}$. To the cooled solution was added 100 g of a 1.0 M tetrapropylammonium hydroxide solution (Aldrich) at $0\text{ }^\circ\text{C}$ dropwise over 2 h. The mixture was then stirred at 80 – $90\text{ }^\circ\text{C}$ for 3–5 h. The mixture was returned to its original volume by the addition of deionized water ($18.0\text{ m}\Omega$, Barnsted E-Pure system) and then transferred to a clean, Teflon-lined autoclave, which was heated to $175\text{ }^\circ\text{C}$ for 3 days. The resulting solid was filtered, rinsed thoroughly with distilled water, and calcined at $500\text{ }^\circ\text{C}$ to remove the organic template.

Characterization. X-ray diffraction (Siemens D500 θ – 2θ diffractometer, Ni-filtered Cu radiation ($K\alpha$)) confirmed that the materials produced were authentic crystalline samples of silicalite and TS-1 by the observation of a characteristic diffraction pattern.⁵ The exact content of titanium in each sample, expressed as a mole percent ($[\text{Ti}]/([\text{Si}] + [\text{Ti}]) \times 100$), was determined by elemental analysis. Samples referred to in the text as 0.5%, 1.5%, and 2.0% titanium had exact concentrations of 0.52, 1.53, and 1.97 mol % titanium, respectively. To assess the purity of the final products, the materials were analyzed by inductively coupled plasma mass spectroscopy (ICP-MS). The instrumentation was a Finnigan MAT Element ICP-MS with a Glass Expansion MicroMist nebulizer. The nebulizer gas flow (Ar) was 1.06 L/min. The cooling gas flow was 13 L/min, and the ICP power was 1300 W. Results: Al, Ga, In, Ge, Pb, Sc, Y, V, Nb, Co, $<1\text{ ppb}$; Na, Li, Sn, Te, Zr, Cr, Ni, Cu, Zn, $<50\text{ ppb}$.

Electronic Spectroscopy. Emission spectroscopy was carried out on a Spex Fluorolog II equipped with 0.22 m double monochromators (Spex 1680) and a 450 W Hg/Xe lamp. Front face (22.5°) collection was used to collect both emission and emission excitation spectra. Cutoff filters were used to suppress second-order excitation lines. It was determined that reproducible emission spectra were attained only after calcination of the samples at $750\text{ }^\circ\text{C}$ under a flow of oxygen (UHP grade) and that it was imperative that they not experience ambient laboratory conditions again prior to data collection. As a result,

they were taken from a tube furnace directly into an antechamber under a dry N_2 purge, where they were mounted in an APD model DE-202 cryostat, shrouded, and evacuated. The samples were carefully aligned to maximize intensity in the detector prior to collection of spectra to ensure the best reproducibility of emission intensities. All reported spectra were corrected for the lamp profile and the detector response. Spectra reported in wavenumber units were corrected in the standard way for the band-pass variability in spectra collected at fixed wavelength resolution.⁷

Vibronic Analysis. Vibrational modes taken from the λ_{\max} of the resolved vibronic bands in the emission spectrum were determined from a spectrum collected at 12 K with 350 nm excitation and 0.25 mm slits. The error in each mode was estimated as that of the instrument resolution, which has a dispersion of 1.70 nm/mm.⁸ At the slit width used, this yields a resolution of 0.85 nm or $\pm 17\text{ cm}^{-1}$ at 20000 cm^{-1} . Since the reported vibrational mode is the difference between two resolved peaks, application of the propagation of error to this difference yields an error of $\pm 24\text{ cm}^{-1}$ for the experimentally determined mode.

Franck–Condon analysis was carried out using a published procedure.⁹ A reduced mass of 12 amu for a Ti–O asymmetric stretch was assumed, the ground- and excited-state vibrational frequencies were taken to be the same ($\nu_g = \nu_e$), and a frequency of 965 cm^{-1} was found to give the best agreement with the data. The normal coordinate change was varied to best reproduce the intensity distribution of the experimentally observed vibronic progression.

Diffuse Reflectance UV–Vis Spectroscopy. The diffuse reflectance UV–vis spectra were collected on a Perkin-Elmer Lambda 900 UV–vis–near-IR spectrophotometer equipped with a 160 mm integrating sphere. The samples were taken from a 500 °C tube furnace into a purged antechamber that also ported to the sample compartment of the N_2 -purged spectrometer. The spectra were collected as total reflectance spectra and displayed in Kubelka–Munk units.¹⁰

Time-Resolved Emission. Fluorescence was induced using 355 nm excitation pulses produced from a frequency-tripled DCR-2a 10 Hz pulsed Nd:YAG laser system with a 9 ns pulse time width and a 8 mm physical diameter. A Jarrel-Ash 0.25 m ($f/3.6$) Ebert monochromator, model 82-410 (Scientific Measurement Systems, Inc.), was the dispersive element prior to the detector, which is a Hamamatsu R928 extended red high-sensitivity side-on-type photomultiplier tube with all dynodes employed. The signal from the PMT was coupled to the oscilloscope with 5.0 k Ω load resistor. A LeCroy model 9410 dual-channel 150 MHz digital oscilloscope was used in the collection and handling of data.

Data analysis was carried out on the emission decays, collected at 274 and 77 K over a range of monitoring wavelengths from 450 to 600 nm. Fits of the overall emission decay curve were carried out using a monoexponential ($I/I_0 = ae^{-t/\tau}$) and a biexponential ($I/I_0 = ae^{-t/\tau} + be^{-t/\tau'}$) decay function, where I is the intensity, t is time, and τ is the lifetime. Decays were fit starting from 5% after the initial spike to avoid convolution with the exciting light. The monoexponential fits were uniformly poor ($R^2 \leq 0.981$), while fits to the biexponential functions were considerably better with $R^2 \geq 0.997$ and 0.998 obtained for the 274 and 77 K data, respectively. Lifetimes collected at 77 K were significantly better due to the increased intensity at that temperature, which yielded better signal-to-noise ratios.

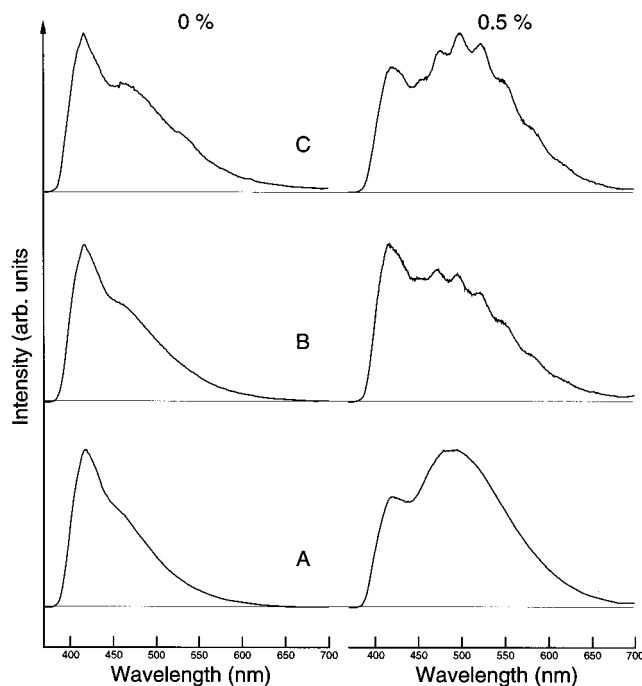


Figure 1. Emission spectra of silicalite (340 nm excitation) and 0.5% TS-1 (350 nm excitation) at (A) room temperature, (B) 77 K, and (C) 12 K.

Results

Luminescence Properties of Silicalite and Titanium Silicalite. The room temperature emission spectra of silicalite and TS-1 (0.5 mol % Ti) are shown in Figure 1A. The pure silicalite sample shows a non-Gaussian emission band with a maximum centered around 417 nm. The band shape is excitation-wavelength-dependent, suggesting that it contains emissions from more than one emitting site. By contrast, TS-1 shows two well-resolved peaks at 422 and 499 nm. Comparison with the control spectrum clearly indicates that the 422 nm band corresponds directly to the intrinsic emission from the silicalite matrix, which suggests that the low-energy emission (499 nm) is particular to TS-1 and, hence, may originate specifically from titanium. As would be expected, the spectra become more intense and better resolved as the temperature decreases (Figure 1). At 77 and 12 K, shoulders at 467 and 545 nm are resolved in the silicalite spectrum along with the sharp peak at 422 nm. For TS-1, the 499 nm band shows evidence of a vibrational progression at 77 K (Figure 1B), which becomes well resolved at 12 K (Figure 1C).

The dependence of the emission spectra of TS-1 on titanium concentration is shown in Figure 2. Two things are evident from this series of spectra. The first is that, consistent with emission from titanium, the intensity of the 499 nm peak increases relative to the 417 nm band as the amount of titanium increases. Second, the vibrational structure observed at low temperature is resolved only in the lower concentrations of titanium.

Analysis of the Vibrational Structure in the Luminescence Peak of TS-1. Figure 3 shows the vibrationally resolved 12 K luminescence spectrum of TS-1 (0.5% Ti) with the frequencies of the resolved modes indicated. Energy differences between each mode in the progression, which correspond to the frequency of the active vibration, were calculated, and an average value of $966 (\pm 24)\text{ cm}^{-1}$ was determined. The infrared spectrum of silicalite shows intense vibrations at 1227, 1105, and 805 cm^{-1} , corresponding to modes of the silica lattice. As titanium is added to the framework to form TS-1, a peak unique to this material

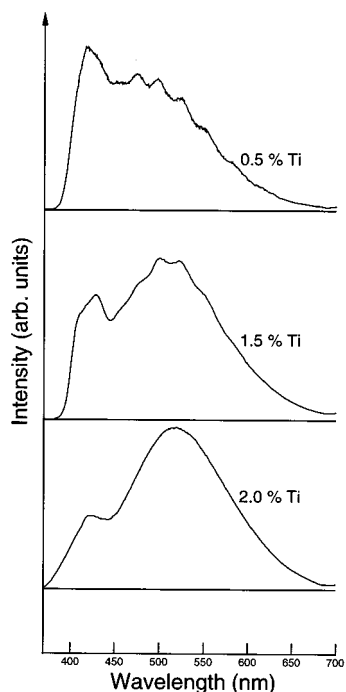


Figure 2. Emission spectra for TS-1 samples containing 0.5, 1.5, and 2 mol % Ti (77 K, 350 nm excitation).

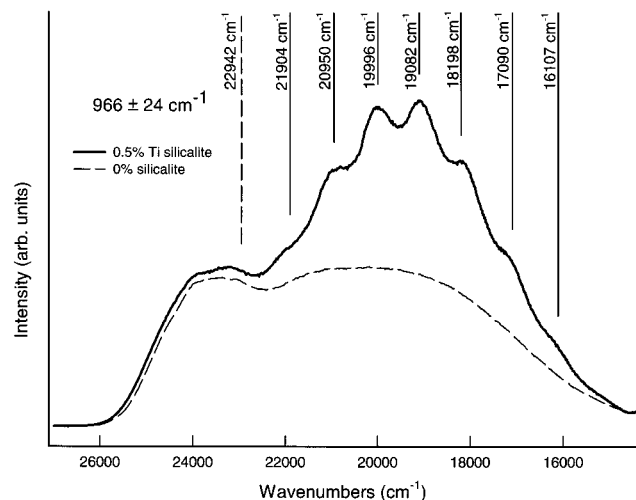


Figure 3. Emission spectra of 0.5% TS-1 (—) and silicalite (---) at 12 K (350 nm excitation). Vibrational frequency is the average of all peaks except 22942 cm^{-1} , which is poorly resolved. Spectra were not scaled. The relative intensities displayed are those recorded.

emerges at $\sim 960 \text{ cm}^{-1}$. This spectral band has been reported previously and, in fact, has been commented on rather extensively.³ It has been assigned to a titanium–silica mode, though more recent arguments have suggested that it is predominantly a silica (SiO^-) mode “perturbed” by the presence of a titanium-(IV) ion.¹¹ Not observable in the infrared spectrum due to interference from the silicalite, but seen in the Raman spectrum, is a titania-related mode at $\sim 1100 \text{ cm}^{-1}$.¹² This peak, however, is much too high in frequency to be a reasonable candidate for the resolved progression. The absence of any other bands in the $850\text{--}1050 \text{ cm}^{-1}$ region of the vibrational spectrum, coupled with the good agreement in energy between the vibronic progression in the emission spectrum and the infrared spectrum, suggests that it can be assigned with considerable certainty to the titania–silica mode.

Photophysical Properties of TS-1. The unambiguous determination of the luminescence lifetime of the titanium emission in TS-1 is complicated by the presence of the overlapping silicalite emission, which contributes to the overall spectrum. Consistent with this, the time-resolved luminescence decays of TS-1 (355 nm excitation, 0.5 mol %) were poorly fit by a monoexponential decay function while a biexponential function yielded significantly better fits as indicated by the R factor and the residuals.¹³ Emission lifetimes for both components are very long, indicating that phosphorescence is occurring from both the titanium and the silicalite. Decay curves were recorded over the emission envelope from 450 to 600 nm. The relative contribution of the two lifetimes (obtained from the preexponential factors of the biexponential fit) to the total emission decay varied systematically over the emission envelope (Table 1). The short-lived component (τ_1) becomes the dominant contribution as the wavelength increases until, at 600 nm, it accounts for about 90% of the total decay. On the basis of this observed trend, we assign the short-lived component to the titanium emission and the longer-lived component to the intrinsic silicalite background emission.

Lifetimes collected at 77 K, which are better determined due to the higher intensity of the emission, indicate that the titanium emission (τ_1) is relatively constant over the emission envelope, giving an average value of $7.48 \pm 0.59 \text{ ms}$ while the long component shows significant variation ($\pm 20\%$). This is consistent with our observation that the silicalite emission appears to contain multiple emitting species.

Electronic Spectroscopy of TS-1. The emission excitation spectrum for TS-1 (0.5% Ti, 12 K), monitored on the red edge of the titanium emission at 600 nm, is shown in Figure 4. The onset of significant intensity occurs at approximately 26700 cm^{-1} and then increases gradually to 35100 cm^{-1} with a resolved shoulder at 31228 cm^{-1} . Above 35000 cm^{-1} the intensity increases sharply to the limits of our excitation range at 40000 cm^{-1} . Importantly, there is measurable intensity over the frequency range from 26000 to 40000 cm^{-1} , indicating that the titanium is being electronically excited throughout this range. Figure 5 shows the electronic absorption spectra, collected as diffuse reflection spectra and plotted in Kubelka–Munk units, for silicalite and for TS-1 containing 0.5% and 1.5% titanium. The spectrum for pure silicalite shows a single strong absorption with a λ_{max} at 46657 cm^{-1} . This spectrum is qualitatively similar to that of TS-1 containing 0.5 mol % titanium, which has a single absorption maximum at 47188 cm^{-1} . In both cases there is no measurable absorption below $\sim 33000 \text{ cm}^{-1}$. At 1.5 mol % titanium, however, detectable spectral intensity begins to appear below 37000 cm^{-1} . The onset of absorption occurs at $\sim 27000 \text{ cm}^{-1}$ and increases gradually until, at $\sim 33500 \text{ cm}^{-1}$, it increases sharply. More importantly, the emission excitation spectrum reproduces well the absorption spectrum in the range between 25000 and 40000 cm^{-1} .

Discussion

Assignment of the Titanium Emission in TS-1. As indicated by the data, the luminescence spectrum of TS-1 consists of two distinct emitting regions: a sharp, high-energy feature centered at 422 nm and a broad low-energy band at 499 nm. The high-energy band can be clearly assigned to intrinsic emission from silicalite itself. The exact origin of the silicalite luminescence is unclear, although the excitation dependence of the band envelope suggests that several emitting species are present. Under the processing conditions employed, this emission is unlikely to contain a significant contribution from adsorbed

TABLE 1: Emission Lifetimes for TS-1

monitoring wavelength (nm)	274 K				77 K			
	τ_1^a	% ^b	τ_2^a	% ^b	τ_1^a	% ^b	τ_2^a	% ^b
450	0.0788	75	0.377	15	7.49	66	7.51	34
500	0.0532	82	0.267	18	7.00	84	19.0	16
550	0.0773	89	0.464	11	8.13	93	48.0	7
600	0.0867	88	0.487	12	8.00	94	62.0	6
average	0.0816 ± 0.021	0.399 ± 0.010	7.66 ± 0.52	34.1 ± 25.2				

^a Lifetimes in milliseconds. ^b Percents represent the contribution to the total decay for each component of the biexponential fit: $\% = (a/(a + b)) \times 100$ and $(b/(a + b)) \times 100$ from $I/I_0 = ae^{-t/\tau_1} + be^{-t/\tau_2}$.

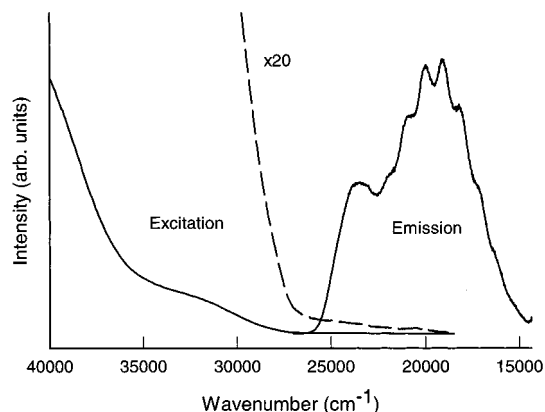


Figure 4. Emission (350 nm excitation) and emission excitation spectra (monitored at 600 nm) of 0.5% TS-1 measured at 12 K.

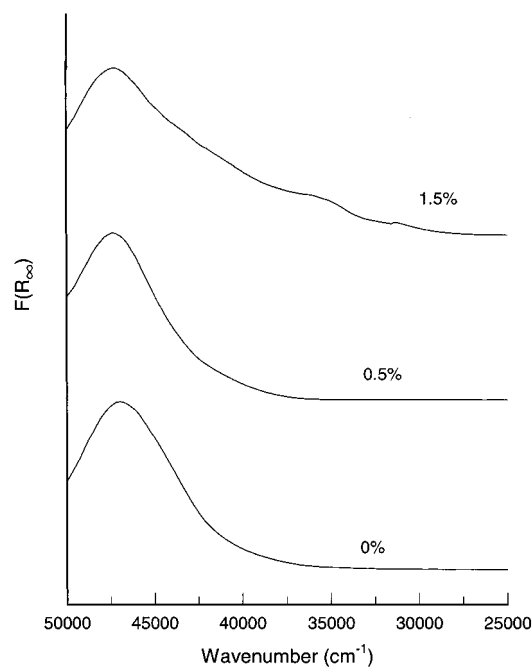


Figure 5. Electronic spectra collected as diffuse reflectance spectra and presented in Kubelka–Munk units for silicalite and 0.5% and 1.5% Ti TS-1.

organic species and, therefore, probably arises from trace metal impurities or from naturally occurring defect sites in the silicalite lattice. The low-energy emission (499 nm) can be assigned with certainty as emanating from the titanium. This assignment is supported by the absence of this band in pure silicalite, the dependence of its relative intensity on titanium concentration, and the observation of vibronic structure in a mode assignable to a Si–O–Ti stretch. The observation and assignment of the titanium emission is important for several reasons. On a fundamental level, it increases our understanding of the

electronic structure and energetics of the reactive sites in these materials. It also allows a critical and quantitative assessment to be made of prior assignments of the structure of the titanium sites in the silicalite lattice based on diffuse reflectance electronic spectroscopy.

There have been two previous reports of luminescence from titanium in TS-1. A note by Ichihashi et. al. reported a single broad emission centered at 455 nm for a sample containing 2% titanium.¹⁴ This spectrum appears, on the basis of our data and analysis, to be an unresolved average between the titanium emission and the silicalite background. A more complete study by Lamberti et. al. on TS-1 (2.03 wt % Ti, collected at room temperature) reported two emissions at 430 and 495 nm.⁴ While the positions of these bands are in close agreement with our observations, they were assigned to two distinct titanium emissions arising from different sites in the silicalite lattice. As we have shown, a careful comparison of the emission data for TS-1 and a titanium-free control (Figure 1) reveals that the high-energy peak is inherent to the silicalite and *only* the low-energy band is attributable to titanium emission. Lamberti et al. disregarded the contribution from the silicalite emission to the luminescence of TS-1 because they observed it to be an order of magnitude weaker than the TS-1 emission. It is well-known that reproducible intensities are extremely difficult to achieve in emission spectra collected from microcrystalline solids.¹⁵ Optical noise caused by random fluctuations in the optical transfer from the scattering media can lead to large variations in the intensity from sample to sample. As can be seen from the overlay in Figure 3, with careful optical alignment, the intensity, position, and shape of this band is completely superimposable on the high-energy emission in TS-1, proving that it contributes significantly to the overall spectrum.¹⁶

While the assignments made in this previous luminescence study are incorrect, the question of how many different titanium sites occur in TS-1 is an important one. There are crystallographically distinct positions for which titanium can potentially substitute for silicon in the lattice. In addition to the lattice sites, there is also the possibility of extraframework and surface species, though recent NMR studies have indicated that most of the titanium resides in lattice sites.¹⁷ If all the sites are emissive and reside in very different coordination environments, then several distinct emission peaks would be expected. Conversely, if the coordination geometries of the emitting sites are very similar, then a single broad, excitation-dependent emission peak might be expected. For the concentration range of titanium investigated, no titanium emission, apart from the 499 nm band, is observed, with all other spectral features being accounted for by the silicalite background. Furthermore, while the intensities of the silicalite background and the titanium emission vary dramatically with respect to each other as a function of excitation wavelength, the 499 nm titanium emission band is itself quite excitation invariant over an excitation range from 280 to 350 nm. In short, notwithstanding the sensitivity

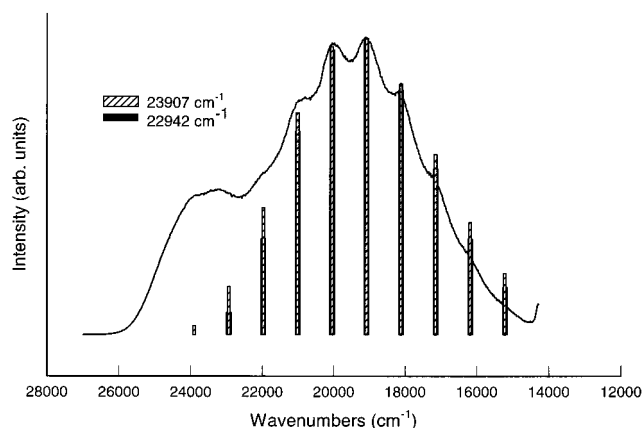


Figure 6. Franck–Condon progression based on $E_{00} = 22942 \text{ cm}^{-1}$ and $E_{00} = 23907 \text{ cm}^{-1}$.

of emission spectroscopy, no clear evidence for multiple titanium emitting sites can be gleaned from the spectra. While this may suggest that only one distinct titanium site emits, such an interpretation is probably not warranted. We cannot, for example, completely rule out the presence of other, weak titanium emissions in the area of spectral congestion imparted by the silicalite background. Alternatively, close similarities in the coordination geometries of the individual sites, irrespective of their crystallographic distinction, may render them indistinguishable in the spectrum. Indeed, the loss of resolvable vibronic structure at higher titanium concentrations may be due to the superposition of closely related emissions emanating from the different sites, although this observation may also be accounted for by changes in the coupled vibrations of the lattice with increasing titanium substitution.

Spectroscopic Assignments and Franck–Condon Analysis.

In the absence of a well-characterized coordination geometry, rigorous spectroscopic assignments are impossible. The fact that the titanium is in the +4 oxidation state means that the excited states are all LMCT in nature. The long lifetime (80 μs at room temperature) coupled with the weakness of the electronic absorption in the region where direct excitation would be expected suggests that the emitting state is strongly nonallowed. The unambiguous assignment of the zero-point energy (E_{00}) of the emitting state is also difficult due to the fact that the silicalite background obscures the high-energy edge of the titanium emission. We expect, on the basis of the position and apparent bandwidth of the emission, that E_{00} should fall between 22000 and 24000 cm^{-1} , underneath the silicalite background. Consistent with this expectation, the excitation spectrum has measurable, albeit weak, intensity in this region (Figure 4). As mentioned, the emitting state is nonallowed and a direct transition into it would be very weak. The highest energy vibronic band that can be determined with confidence is at $\sim 21904 \text{ cm}^{-1}$ (Figure 4). At higher energy there appears to be another mode of the progression, which can be seen as a shoulder on the red edge of the silicalite emission at $\sim 23000 \text{ cm}^{-1}$. While this peak is in a reasonable position to be the origin of the progression, it is certainly possible that other modes lie to higher energy and are obscured.

If we assign the mode at $\sim 23000 \text{ cm}^{-1}$ as either the 0–0 or the 0–1 mode, then the most intense and best resolved vibrational mode in the center of the envelope at 19082 cm^{-1} would be the 0–4 or 0–5 transition. If we start from that point and add four and five 965 cm^{-1} quanta, we estimate a zero-point energy of either 22942 or 23907 cm^{-1} , respectively. Figure 6 shows the Franck–Condon progressions calculated for a 965

cm^{-1} mode originating from each of these estimated origins. Regardless of the origin, very good agreement is obtained between the observed and calculated progressions, further supporting our vibronic assignment. As can be seen from the spectrum, progressions generated at both origins give a good reproduction of the intensity distribution of the unobscured part of the spectrum, though better agreement is obtained with the low-energy edge of the emission from the progression originating at 22942 cm^{-1} .¹⁸ The normal coordinate change required to generate either of these progressions is reasonable, with values of 0.17 and 0.19 \AA used for the 22942 and 23907 cm^{-1} origins, respectively. A Franck–Condon progression generated for an origin one additional mode to higher energy (24872 cm^{-1}) proved to be much poorer at reproducing the spectrum, even with large values for the normal coordinate change. This, coupled with the fact that this origin would lie well under the onset of absorption, suggests that it is probably not a reasonable candidate for E_{00} .

In general, the spectroscopic and photophysical properties of the titanium in TS-1 are analogous to those observed for other high-valent early transition metals in a silica matrix. In particular, both vanadium(V) and chromium(VI) dispersed in amorphous silica have long-lived phosphorescent LMCT states, and both show resolved vibronic progressions in the emission spectra corresponding to M–O–Si stretching modes.^{19,20} Taken as a series, the emission energy decreases going from titanium to chromium as the metal becomes easier to reduce. While it is not possible to infer molecular structure from such an analogy, the similarities are striking enough to suggest that perhaps some particular structural feature, common to all of these metal sites, gives rise to the observed spectroscopic and photophysical properties.

Electronic Spectroscopy and the Assignment of Ti Coordination Geometry. Since the discovery of TS-1 (and related titania–silica materials), a great deal of effort has been expended to elucidate the coordination geometry of the titanium center. X-ray analyses (XAFS and XANES) clearly indicate that the titanium is not octahedral, with coordination numbers of 4–5 usually being reported.³ The initial suggestion that titanyl groups (T=O) are present has been disputed by a number of investigators, and the current view is that Ti(IV) is substituted isomorphically for Si(IV) in the silica network and resides in a tetrahedral or distorted tetrahedral environment.^{21–23}

Among the arguments used to support the assignment of tetrahedral coordination to the titanium sites in TS-1 are those based on diffuse reflectance UV–vis spectroscopy. As a result, this technique has grown to serve as a general analytical tool for determining the presence of extraframework titania in samples of TS-1.^{24–27} The basis of these structural arguments, as put forth by Bocutti et al., involves an application of Jürgensen’s concept of optical electronegativity.²⁴ In employing this approach, the energy (ν (cm^{-1})) of a LMCT transition is predicted from the optical electronegativity equation (shown below), where $\chi(\text{M})$ is a function of the metal and its coordination geometry and $\chi(\text{L})$ is a function of the ligand.^{28,29}

$$\nu (\text{cm}^{-1}) = 30000[\chi(\text{L}) - \chi(\text{M})]$$

In the analysis of TS-1, the value of $\chi(\text{M})$ used for titanium(IV) was 2.05 and 1.85 for octahedral and tetrahedral coordination, respectively, and $\chi(\text{L})$ for the oxide ligand was estimated at 3.45.³⁰ These values predict a LMCT transition at 48000 cm^{-1} for tetrahedral coordination and 42000 cm^{-1} for octahedral coordination. The authors concluded from these predictions and the absence of an observable absorption in the diffuse reflectance

between 30000 and 42000 cm^{-1} that the titanium did not sit in an octahedral site. While this is a reasonable conclusion, it is more compellingly deduced from X-ray data.³¹ The authors further concluded that the “remarkable” agreement between the energies of the experimentally determined absorption maximum and the predicted maximum proves that the titanium is in a tetrahedral environment in the silicalite lattice.²⁴

There is a fundamental problem with this argument that can be addressed with the spectroscopic data reported here. The optical electronegativity expression predicts the energy of the LMCT transitions for only two high-symmetry geometries: tetrahedral and octahedral. However, it cannot be used to exclude other, lower symmetry coordination environments that could easily have LMCT transitions at the same energy as the high-symmetry species. More importantly, it is clear from the spectroscopy that the primary assertion that no electronic absorption is observed below 42000 cm^{-1} for the titanium site in TS-1 is simply incorrect.^{24,25} The emission excitation spectra clearly show that the emitting state of the titanium is excited at wavelengths between 32000 and 42000 cm^{-1} . The reason that absorption bands in the diffuse reflectance electronic spectrum corresponding to these transitions are not observed until higher concentrations of titanium are reached is due to the weakness of the transitions (which are strongly nonallowed), coupled with the inherent insensitivity of diffuse reflectance techniques.³² These results clearly show that electronic spectroscopy *does not* support simple tetrahedral coordination of the titanium in silicalite. Furthermore, it is not possible to infer a structure from the electronic spectroscopy, though, consistent with X-ray analysis, a lower symmetry, four-coordinate species may very well explain the spectra. It also indicates that the observation of intensity in the diffuse reflection spectrum in the region below 42000 cm^{-1} may not necessarily be diagnostic of extraframework titania, especially in samples with higher titanium concentrations where the weak titanium-based transitions become observable. Conversely, the observation of a strong absorption in that spectral region, especially at lower titanium concentrations, is unlikely to be from the titanium site and may be indicative of extraframework titania or other impurities. Finally, with regard to the resolved vibrational structure, it is clear that the ~ 960 cm^{-1} vibrational mode in TS-1 is not accurately described as a Si–O[−] stretch “perturbed” by the Ti(IV), as has been suggested.^{11,25,33} The fact that it is an active progression in the emission spectrum indicates that it is strongly coupled to the electronic manifold of the titanium and is more correctly viewed as a Ti–O–Si stretch. Notably, recent vibrational studies of crystalline titanium silicates tend to support this interpretation.³⁴

Conclusion

The titanium site in TS-1 catalyst materials has a long-lived phosphorescent excited state with a maximum at 490 nm in the near-UV. This state is significantly lower in energy than was previously suggested by diffuse reflectance absorption spectroscopy. Emission excitation spectra indicate that there are weak electronic absorptions throughout the spectral region from ~ 23000 to 48000 cm^{-1} . These observations bring into question long-standing structural arguments for the coordination of titanium in the silicalite lattice that have been made using electronic spectroscopy.

Acknowledgment. We thank Dr. Eric Lochner of the Materials Research and Technology Center (MARTECH) at Florida State University for providing X-ray analysis and Dr.

David Gormin for his assistance in determining the phosphorescence lifetimes. We thank Dr. Ted Zateslo and Dr. Afi Sachi-Kocher of the National High Magnetic Field Laboratory for assistance with the ICP-MS measurements. We thank Dr. Bruno Notari for helpful discussions. The work was conducted under support provided by the National Science Foundation, Division of Materials Research, under Grant DMR-9623570.

References and Notes

- (1) Nordberg, M. E. U.S. Patent 2326059, 1943.
- (2) Notari, B. *Adv. Catal.* **1996**, *41*, 253.
- (3) Vayssilov, G. N. *Catal. Rev. Sci. Eng.* **1997**, *39*, 219.
- (4) Lamberti, C.; Bordiga, S.; Arduino, D.; Zecchina, A.; Geobaldo, F.; Spano, G.; Genomi, F.; Villian, F.; Vlaic, G. *J. Phys. Chem. B* **1998**, *102*, 6382.
- (5) Taramasso, M. U.S. Patent 4410501, 1983.
- (6) Van Der Pol, A. J. H. P.; van Hoof, J. H. C. *Appl. Catal., A* **1992**, *92*, 93.
- (7) Lakowicz, J. R. *Principles of Fluorescence Spectroscopy*; Plenum: New York, 1983; p 42.
- (8) Ingle, J. D.; Crouch, S. R. *Spectrochemical Analysis*; Prentice Hall: Upper Saddle River, NJ, 1988; p 71.
- (9) McCoy, E. F.; Ross, I. G. *Aust. J. Chem.* **1962**, *15*, 573.
- (10) Blitz, J. P. In *Modern Techniques in Applied Molecular Spectroscopy*; Mirabella, F. M., Ed.; Wiley: New York, 1998; p 189.
- (11) Zecchina, A.; Spoto, G.; Bordiga, S.; Padovan, M.; Leofanti, G.; Petrini, G. In *Catalysis and Adsorption of Zeolites*; Ohlmann, G., Ed.; Elsevier: Amsterdam, 1991; p 671.
- (12) Deo, G.; Turek, A. M.; Wachs, I. E.; Huybrechts, D. R. C. *Zeolites* **1993**, *13*, 365.
- (13) We obtain good fits to a biexponential decay function which accounts well for the two emitting regions in this system. Closer analysis is likely to reveal that the decay is more complex and better fit to a distribution function, as is well-known in heterogeneous porous media. [For a lucid discussion of decays in heterogeneous porous solids see: Castellano, F.; Meyer, G. J. In *Progress in Inorganic Chemistry*; Karlin, K. D., Ed.; Wiley: New York, 1997; Vol. 44, p 167 and references therein.]
- (14) Ichihashi, Y.; Yamashita, H.; Anpo, M.; Souma, Y.; Matsumura, Y. *Catal. Lett.* **1998**, *53*, 207.
- (15) Hurtubise, R. J. *Solid Surface Luminescence Analysis*; Marcel Dekker: New York, 1981; p 60.
- (16) Lamberti et al. [ref 13] also report an emission centered at 500 nm for the tetrahedral model compound $\text{Ti}(\text{OSi}(\text{CH}_3)_3)_4$. This observation was used to assign the low-energy band as originating from a tetrahedral site in the lattice. We observed no emission from this compound either in cyclohexane at room temperature or in a methylcyclohexane glass at 77 K.
- (17) Labouriau, A.; Ott, K. C.; Rau, J.; Earl, W. L. *J. Phys. Chem. B* **2000**, *104*, 5890.
- (18) Better agreement can be realized by relaxing the constraint that $\nu_g = \nu_e$ [Yersin, H.; Otto, H.; Zink, J. I.; Gliemann, G. *J. Am. Chem. Soc.* **1980**, *102*, 951]; however, given the complexity of the spectra and the qualitative nature of this Franck–Condon analysis, this higher level of calculation seems unwarranted.
- (19) Hazenkamp, M. F.; Blasse, G. *J. Phys. Chem.* **1992**, *96*, 3442.
- (20) Tran, K.; Hanning-Lee, M. A.; Biswas, A.; Stiegman, A. E.; Scott, G. W. *J. Am. Chem. Soc.* **1995**, *117*, 2618.
- (21) Notari, B. In *Studies in Surface Science and Catalysis 37*; Grobet, J. M., Ed.; Elsevier: Amsterdam, 1988; p 413.
- (22) Perego, G.; Bellussi, G.; Corno, C.; Taramasso, M.; Buonomo, F.; Esposito, A. In *Studies in Surface Science and Catalysis 28*; Murakami, Y., Iijima, A., Ward, J. W., Eds.; Elsevier: Amsterdam, 1986; p 129.
- (23) Crocker, M.; Herold, R. H. M.; Roosenbrand, B. G.; Kees, A. E.; Wilson, A. E. *Colloids Surf., A* **1998**, *139*, 351.
- (24) Boccuti, M. R.; Rao, K. M.; Zecchina, A.; Leofanti, G.; Petrini, G. In *Structure and Reactivity of Surfaces*; Norterra, C., Zecchina, A., Costa, G., Eds.; Elsevier: Amsterdam, 1989; p 133.
- (25) Zecchina, A.; Spoto, G.; Bordiga, S.; Ferrero, A.; Petrini, G.; Leofanti, G.; Padovan, M. In *Zeolite Chemistry and Catalysis*; Jacobs, P. A., Ed.; Elsevier: Amsterdam, 1991; p 251.
- (26) Geobaldo, F.; Bordiga, S.; Zecchina, A.; Giamello, E.; Leofanti, G.; Petrini, G. *Catal. Lett.* **1992**, *16*, 109.
- (27) Duprey, E.; Beauvier, P.; Springuel-Huet, M.-A.; Bozon-Verduraz, F.; Fraissard, J.; Manoli, J.-M.; Brégeault, J.-M. *J. Catal.* **1997**, *165*, 22.

(28) Jørgensen, C. K. In *Progress in Inorganic Chemistry*; Lippard, S. J., Ed.; Wiley: New York, 1979; p 101.

(29) Lever, A. B. P. *Inorganic Electronic Spectroscopy*; Elsevier: Amsterdam, 1984; p 218.

(30) While this value of the optical electronegativity for the oxo ligand is probably reasonable, it should be noted that there are a number of problems in assigning optical electronegativities for oxygen [Muller, A.; Diemann, E.; Jørgensen, C. K. *Struct. Bonding* **1973**, 14, 23].

(31) On, D. T.; Bonneviot, L.; Bittar, A.; Sayari, A.; Kaliaguine, S. *J. Mol. Catal.* **1992**, 74, 233.

(32) Reference 10, p 188.

(33) Cambor, M. A.; Corma, A.; Perez-Pariente, J. *J. Chem. Soc., Chem. Commun.* **1993**, 557.

(34) Su, Y.; Balmer, M. L.; Bunker, B. C. *J. Phys. Chem. B* **2000**, 104, 8160.